Journal of
Risk and Financial Management

Article

On the Kavya–Manoharan–Burr X Model: Estimations under Ranked Set Sampling and Applications

Osama H. Mahmoud Hassan [1,*], Ibrahim Elbatal [2], Abdullah H. Al-Nefaie [1] and Mohammed Elgarhy [3]

1 Department of Quantitative Methods, School of Business, King Faisal University, Al-Ahsa 31982, Saudi Arabia
2 Department of Mathematics and Statistics, College of Science, Imam Mohammad Ibn Saud Islamic University (IMSIU), Riyadh 11564, Saudi Arabia
3 The Higher Institute of Commercial Sciences, Al Mahalla Al Kubra, Algarbia 31951, Egypt
* Correspondence: ohhassan@kfu.edu.sa

Abstract: A new two-parameter model is proposed using the Kavya–Manoharan (KM) transformation family and Burr X (B_X) distribution. The new model is called the Kavya–Manoharan–Burr X (KMB_X) model. The statistical properties are obtained, involving the quantile (Q_U) function, moment (M_Os), incomplete M_Os, conditional M_Os, M_O-generating function, and entropy. Based on simple random sampling (S_iR_S) and ranked set sampling (R_aS_S), the model parameters are estimated via the maximum likelihood (ML_L) method. A simulation experiment is used to compare these estimators based on the bias (B_I), mean square error (M_SE_R), and efficiency. The estimates conducted using R_aS_S tend to be more efficient than the estimates based on S_iR_S. The importance and applicability of the KMB_X model are demonstrated using three different data sets. Some of the useful actuarial risk measures, such as the value at risk and conditional value at risk, are discussed.

Keywords: KM transformation family; Burr X distribution; moments; entropy; approach of maximum likelihood

check for updates

Citation: Hassan, Osama H. Mahmoud, Ibrahim Elbatal, Abdullah H. Al-Nefaie, and Mohammed Elgarhy. 2023. On the Kavya–Manoharan–Burr X Model: Estimations under Ranked Set Sampling and Applications. *Journal of Risk and Financial Management* 16: 19. https://doi.org/10.3390/jrfm16010019

Academic Editors: Liqun Wang and Klaus Pötzelberger

Received: 10 November 2022
Revised: 19 December 2022
Accepted: 22 December 2022
Published: 28 December 2022

1. Introduction

Burr (1942) proposed twelve types of cumulative distribution functions (cdfs) for modeling lifespan data. The most common of these distributions are the B_X and Burr type XII distributions. The fact that the B_X distribution has a declining and growing hazard function is one of its key characteristics. The B_X distribution has been used extensively in reliability research, agriculture, biology, and medicine. It may also be used to successfully represent strength data as well as to general lifespan data. Many researchers have examined several features of the B_X distribution in recent years; for example, Surles and Padgett (2001) proposed a scaled B_X distribution inference for reliability and stress–strength measurements. Aludaat et al. (2008) studied B_X distribution parameter estimates for grouped data. Furthermore, Raqab and Kundu (2006) created a two-parameter B_X distribution that is a closed variant of the generalized Rayleigh distribution and utilized it to simulate ball bearing data. Algarni et al. (2021) proposed the type I half-logistic Burr XG family and the bivariate Burr X generator of distributions, which were investigated by El-Morshedy et al. (2020). Bantan et al. (2021) discussed the truncated Burr X-G family of distributions. The cdf of the B_X distribution is provided via the following equation:

$$G_{B_X}(x,\alpha,\beta) = \left[1 - e^{-(\alpha x)^2}\right]^{\beta}, x,\alpha,\beta > 0, \quad (1)$$

where α and β are positive scale and shape parameters, respectively. The associated density function (pdf) and hazard rate function (hrf) are respectively supplied with:

$$g_{B_X}(x,\alpha,\beta) = 2\beta\alpha^2 x e^{-(\alpha x)^2}\left[1 - e^{-(\alpha x)^2}\right]^{\beta-1}. \quad (2)$$

and

$$h_{B_X}(x,\alpha,\theta) = \frac{2\beta\alpha^2 x e^{-(\alpha x)^2}\left[1-e^{-(\alpha x)^2}\right]^{\beta-1}}{\left[1-e^{-(\alpha x)^2}\right]^{\beta}} \tag{3}$$

Depending on the shape parameter, the hrf of a B_X distribution could be either a bathtub function or an increasing function. When $\beta \leq \frac{1}{2}$, the hrf is a bathtub shape, and when $\beta > \frac{1}{2}$, the hrf is growing. Surles and Padgett (2005) demonstrated that the two-parameter B_X distribution may be employed in modeling both strength and general lifespan data.

Statistical and applied academics are increasingly interested in constructing flexible lifespan models to improve the modeling of survival data. As a result, substantial work has been performed to generalize several well-known lifespan models, which have been successfully applied to difficulties in a wide range of scientific fields of study. Despite the fact that extra parameters give greater freedom, they also increase the complexity of the parameter estimation. Kumar et al. (2015) proposed a DUS (Dinesh–Umesh–Sanjay) transformation to produce a new parsimonious class of distributions to acquire new lifetime distributions. If G(x) is the baseline cdf, the DUS transformation yields the new cdf F(x), as shown below.

$$F(x) = \frac{e^{G(x)}-1}{e-1}. \tag{4}$$

The merit of using this transformation is that the resulting distribution retains the attribute of being parameter-sparse because no more parameters are added. Kavya and Manoharan (2020) proposed a generalized lifespan model based on the DUS transformation. The generalized DUS (GDUS) transformation's cdf is provided via the following equation:

$$F(x;\alpha,\zeta) = \frac{\exp(G^{\alpha}(x;\zeta))-1}{e-1}, x > 0, \tag{5}$$

where $\alpha > 0$. The associated pdf is supplied with:

$$f(x;\alpha,\zeta) = \frac{\alpha g(x;\zeta)G^{\alpha-1}(x;\zeta)\exp(G^{\alpha}(x;\zeta))}{e-1} \tag{6}$$

where $G(x;\zeta)$ is the baseline distribution and $g(x;\zeta)$ is the parent pdf in the GDUS family. Because it is obviously a transformation rather than a generalization, it will yield a parsimonious distribution in terms of the computation and interpretation because it never contains any additional parameters other than those involved in the baseline distribution. Alotaibi et al. (2022b) proposed bivariate step stress accelerated life tests for the Kavya–Manoharan exponentiated Weibull model under a progressive censoring scheme. Alotaibi et al. (2022a) proposed the Kavya–Manoharan inverse-length biased exponential distribution under a progressive stress model based on progressive type-II censoring.

Recently, Kavya and Manoharan (2021) introduced a new transformation family, called the KM transformation family of distributions. The cdf is provided via:

$$F_{KM}(x) = \frac{e}{e-1}\left(1-e^{-G(x)}\right), x > 0. \tag{7}$$

The associated pdf is supplied with:

$$f_{KM}(x) = \frac{e}{e-1} g(x) e^{-G(x)}, \tag{8}$$

and the hrf is:

$$h_{KM}(x) = \frac{g(x)e^{1-G(x)}}{e^{1-G(x)}-1}. \tag{9}$$

Using a given baseline distribution, this family generates new lifespan models or distributions. They do not add any extra parameters to the model to keep it tuned to the current uncertainty, instead focusing on modeling the lifetime with a process that produces correct parsimonious findings. They chose the exponential and Weibull distributions as baseline distributions because they are widely used in reliability theory and survival analyses.

As our object in this article, we propose a new extension of the BX model based on the KM transformation family called the Kavya–Manoharan B_X (KMB_X) model. A battery of general features of the KMB_X model is discussed. The KMB_X model is developed using the maximum likelihood (ML) technique. It is applied to fit three data sets of biomedical and financial data. Using standard benchmarks, we reveal that it performs better than the selected competing models. The section of actuarial measures concerns useful risk measures, with a focus on the value at risk and conditional value at risk.

The remainder of the article is as follows. The second section presents the KMB_X distribution as well as the density function expansion. Section 3 derives the Q_U function, median, M_Os, incomplete M_Os, M_O-generating function, conditional M_Os, mean residual lifetime, and Rényi entropy. Section 4 employs ML_L estimates under S_iR_S and R_aS_S. In the same section, the simulation experiment is used to compare these estimators based on the B_I, M_SE_R, and efficiency. In Section 5, we highlight the significance of the existing model by studying real data applications to convey its efficiency and applicability. Some useful actuarial risk measures, such as the value at risk and conditional value at risk, are discussed in Section 6. Finally, the concluding remarks are mentioned in Section 7.

2. Kavya-Manoharan Burr X Distribution

We consider $G(x)$ in Equation (7) to be the cdf of the Burr type X distribution given in Equation (1), so that the cdf of the KMB_X distribution can be expressed as:

$$F_{KMB_X}(x;\alpha,\beta) = \frac{e}{e-1}\left(1 - e^{-\left[1-e^{-(\alpha x)^2}\right]^{\beta}}\right). \tag{10}$$

The corresponding pdf and hrf are provided via:

$$f_{KMB_X}(x;\alpha,\beta) = \frac{2e\beta\alpha^2}{e-1} x e^{-(\alpha x)^2}\left[1 - e^{-(\alpha x)^2}\right]^{\beta-1} e^{-\left[1-e^{-(\alpha x)^2}\right]^{\beta}}, \tag{11}$$

and:

$$h_{KMB_X}(x;\alpha,\beta) = \frac{2e\beta\alpha^2}{e-1} x e^{-(\alpha x)^2}\left[1 - e^{-(\alpha x)^2}\right]^{\beta-1} e^{-\left[1-e^{-(\alpha x)^2}\right]^{\beta}} \times \frac{1}{\frac{e}{e-1}\left(1-e^{-\left[1-e^{-(\alpha x)^2}\right]^{\beta}}\right)}. \tag{12}$$

Using the generalized binomial $(1-z)^{b-1} = \sum_{j=0}^{\infty}(-1)^j \binom{b-1}{j} z^j, |z| < 1$ and $e^{-x} = \sum_{i=0}^{\infty}\frac{(-x)^i}{i!}$, the expansion of the pdf in (11) may be expressed as below:

$$f_{KMB_X}(x;\alpha,\beta) = \sum_{i,j=0}^{\infty} \varpi_{i,j} x e^{-(j+1)(\alpha x)^2}, \tag{13}$$

where:

$$\varpi_{i,j} = \frac{2e\beta\alpha^2}{e-1}\frac{(-1)^{i+j}}{i!}\binom{\theta(i+1)-1}{j}. \tag{14}$$

Hereafter, a random variable X that has the pdf from (11) is symbolized by $X \backsim KMB_X(\alpha,\beta)$. Figures 1 and 2 show the curves for the pdf and hazard rate function of the KMB_X distribution.

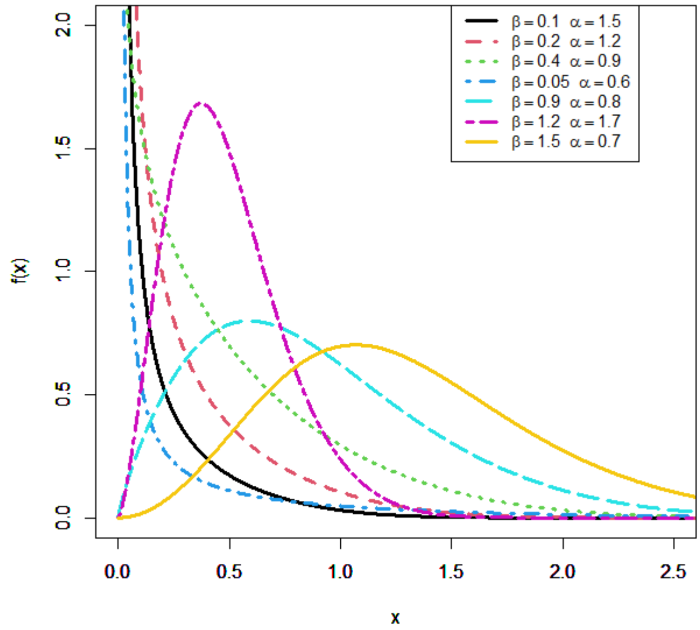

Figure 1. The pdf plots of the KMB_X model.

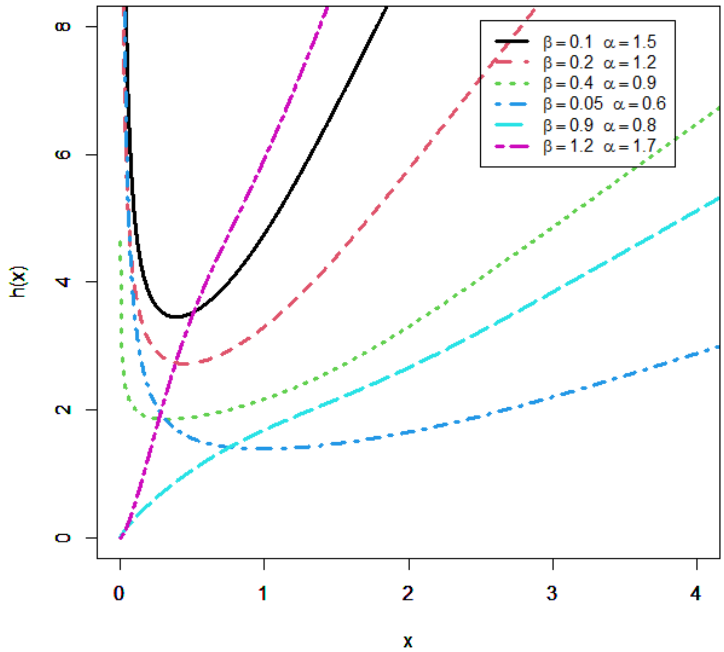

Figure 2. The hrf plots of the KMB_X model.

3. Statistical Measures

In this section, we give some important statistical properties of the KMB_X distribution, such as the Q_U function, median, M_Os, incomplete M_Os, M_O-generating function, conditional M_Os, mean residual lifetime, and Rényi entropy.

3.1. Quantile Function

The p^{th} Q_U function of the KMB_X distribution is supplied with:

$$x_p = Q(p) = -\frac{1}{\alpha} log\left\{1 - \left[-log\left(1 - p\left(1 - e^{-1}\right)\right)\right]^{\frac{1}{\beta}}\right\}^{\frac{1}{2}}, \tag{15}$$

where $p \in (0,1)$. Additionally, when we put p = 0.5, we can get the median as below:

$$Median = -\frac{1}{\alpha} log\left\{1 - \left[-\log\left(1 - 0.5\left(1 - e^{-1}\right)\right)\right]^{\frac{1}{\beta}}\right\}^{\frac{1}{2}} \tag{16}$$

3.2. Moments and Incomplete Moments

The statistical moments of different orders are important to define the uncertainty characteristics of the distributions. Using the expansion of (13), the r_{th} M_O of X is provided via:

$$\mu'_r = \int_{-\infty}^{\infty} x^r f(x)dx = \sum_{i,j=0}^{\infty} \varpi_{i,j} \int_0^{\infty} x^{r+1} e^{-(j+1)(\alpha x)^2} dx \tag{17}$$

setting $y = (j+1)(\alpha x)^2$, after using algebra, the r_{th} M_Os is provided with:

$$\mu'_r = \sum_{i,j=0}^{\infty} \varpi_{i,j} \frac{\Gamma\left(\frac{r}{2}+1\right)}{2\alpha^{r+2}(j+1)^{\frac{r}{2}+1}}. \tag{18}$$

Individually, the first four moments are obtained by setting r = 1, 2, 3, and 4 in (18). Additionally, the rth central moment (μ_r) of X is given by:

$$\mu_r = E(X - \mu'_1)^r = \sum_{i=0}^{r} (-1)^i \binom{r}{i} (\mu'_1)^i \mu'_{r-i}. \tag{19}$$

The skewness (SK) and kurtosis (Ku) are defined by:

$$SK = \frac{\mu_3}{\mu_2^{3/2}}, Ku = \frac{\mu_4}{\mu_2^2}. \tag{20}$$

The s_{th} incomplete M_O of the KMB_X distribution is expressed by:

$$\eta_s(t) = E(X^s|X < t) = \int_0^t x^s f(x)dx \tag{21}$$

We can write the following equation from Equation (12):

$$\eta_s(t) = \sum_{i,j=0}^{\infty} \varpi_{i,j} \frac{\gamma\left(\frac{s}{2}+1, (j+1)(\alpha t)^{\beta}\right)}{2\alpha^{s+2}(j+1)^{\frac{s}{2}+1}}, \tag{22}$$

where $\gamma(s,t) = \int_0^t x^{s-1}e^{-x}dx$ is the lower incomplete gamma function.

3.3. Conditional Moments

For the KMB_X distribution, it is easy to note that the conditional M_Os $E(X^s|X\rangle t)$ can indeed be expressed as:

$$E(X^s|X\rangle t) = \frac{1}{\overline{F}(t)} H_s(x), \tag{23}$$

where:

$$\begin{aligned} H_s(x) &= \int_t^{\infty} x^s f(x)dx \\ &= \sum_{i,j=0}^{\infty} \varpi_{i,j} \frac{\Gamma\left(\frac{s}{2}+1,(j+1)(\alpha t)^{\beta}\right)}{2\alpha^{s+2}(j+1)^{\frac{s}{2}+1}}, \end{aligned} \tag{24}$$

and $\Gamma(s,t) = \int_t^{\infty} x^{s-1}e^{-x}dx$ is the upper incomplete gamma function. An important application of the conditional M_Os is the mean residual life (MRL) function. It is very important in terms of reliability and survival analyses, and it is used to model the burn-in and conservation of the component. For the KMB_X distribution, the MRL function in terms of the first conditional M_O is:

$$\mu(t) = E((X - t)|X\rangle t) = \frac{1}{\overline{F}(t)} H_1(x) - t, \quad (25)$$

where $H_1(x)$ is the first complete M_Os following from (24) with $s = 1$. Another application is the mean deviations about the mean μ and the median. They are used to measure the spread in a population from the center. The mean deviations about the mean and about the median are defined by $\delta_\mu = 2\mu\ F(\mu) - 2\mu + 2H_1(\mu)$ and $\delta_M = 2H_1(M) - \mu$, respectively, where $F(\mu)$ is evaluated from (10), $H_1(\mu)$ and $H_1(M)$ can be obtained from (24).

3.4. Moment-Generating Functions

The M_O-generating function of the KMB_X distribution can indeed be expressed as:

$$\begin{aligned} M_X(t) = E\left(e^{tX}\right) &= \int_0^\infty e^{tx} f(x)dx = \sum_{r=0}^{\infty} \tfrac{t^r}{r!} \mu'_r \\ &= \sum_{i,j,r=0}^{\infty} \tfrac{t^r}{r!} \varpi_{i,j} \frac{\Gamma\left(\frac{r}{2}+1\right)}{2\alpha^{r+2}(j+1)^{\frac{r}{2}+1}}. \end{aligned} \quad (26)$$

3.5. Rényi Entropy

The Rényi entropy is provided via:

$$I_R(\delta) = \frac{1}{1-\zeta} log\left[\int_0^\infty f^{\,\delta}(x)dx\right],\ \rho > 0,\ \rho \neq 1. \quad (27)$$

The Rényi entropy of X can indeed be expressed as:

$$I_R(\delta) = \frac{1}{1-\delta} log\left\{\left(\frac{e\beta\alpha^2}{e-1}\right)^{\delta} \sum_{i,j=0}^{\infty} \frac{2^{\delta-1}(-1)^{i+j}\Gamma\left(\frac{\delta+1}{2}\right)}{i![(j+\delta)\alpha^2]^{\frac{\delta+1}{2}}}\right\}. \quad (28)$$

4. Parameter Estimation

The ML_L estimate of the KMB_X model parameters is derived in this part using R_aS_S and R_aS_S. A simulation study is also carried out to compare the behavior of the estimators for both approaches.

4.1. ML_L Approach under S_iR_S

We use the ML_L estimates (ML_LE_s) approach to estimate the unknown parameters of the KMB_X distribution in this part. We assume that $\boldsymbol{x_1, \ldots, x_n}$ is an $\boldsymbol{n}$-th random sample (R_S) from the KMB_X distribution provided by (11). The KMB_X distribution's log-likelihood (log-L_L) (L) function is provided via

$$\begin{aligned} \boldsymbol{L} = \boldsymbol{n}\mathbf{log}\left(\tfrac{\mathbf{2e}}{\boldsymbol{e}-\mathbf{1}}\right) + \boldsymbol{n}\mathbf{log}(\boldsymbol{\beta}) + 2\boldsymbol{n}\mathbf{log}(\boldsymbol{\alpha}) + \sum_{\boldsymbol{i}=\mathbf{1}}^{\boldsymbol{n}} \mathbf{log}(\boldsymbol{x_i}) - \boldsymbol{\alpha}^{\mathbf{2}} \sum_{\boldsymbol{i}=\mathbf{1}}^{\boldsymbol{n}} \boldsymbol{x_i} \\ - \textstyle\sum_{i=1}^{n}\left[1 - e^{-(\alpha x_i)^2}\right]^{\beta} + (\beta - 1)\sum_{i=1}^{n} \log\left[1 - e^{-(\alpha x_i)^2}\right]. \end{aligned} \quad (29)$$

Differentiating Equation (29) partially with regard to $\boldsymbol{\alpha}$ and $\boldsymbol{\beta}$ to equate the results to 0, we get the following:

$$\begin{aligned} \tfrac{\partial \boldsymbol{L}}{\partial \boldsymbol{\alpha}} = \tfrac{\mathbf{2n}}{\boldsymbol{\alpha}} - \mathbf{2}\boldsymbol{\alpha} \sum_{\boldsymbol{i}=\mathbf{1}}^{\boldsymbol{n}} (\boldsymbol{x_i}) - \mathbf{2}\boldsymbol{\alpha\beta} \sum_{\boldsymbol{i}=\mathbf{1}}^{\boldsymbol{n}} \boldsymbol{x_i^2 e^{-(\alpha x_i)^2}} \left[\mathbf{1} - \boldsymbol{e^{-(\alpha x_i)^2}}\right]^{\boldsymbol{\beta}-\mathbf{1}} + \\ (\boldsymbol{\beta} - \mathbf{1}) \sum_{\boldsymbol{i}=\mathbf{1}}^{\boldsymbol{n}} \tfrac{\mathbf{2}\boldsymbol{\alpha x_i^2 e^{-(\alpha x_i)^2}}}{\mathbf{1} - \boldsymbol{e^{-(\alpha x_i)^2}}}, \end{aligned} \quad (30)$$

and:

$$\frac{\partial L}{\partial \beta} = \frac{n}{\beta} - \sum_{i=1}^{n}\left[1 - e^{-(\alpha x_i)^2}\right]^{\beta}\log\left[1 - e^{-(\alpha x_i)^2}\right] + \sum_{i=1}^{n}\log\left[1 - e^{-(\alpha x_i)^2}\right]. \tag{31}$$

The ML_LE_s of parameters α and β symbolized by $\hat{\alpha}$ and $\hat{\beta}$, respectively, are investigated by solving the above non-linear system of equations simultaneously. As a result, we cannot get specific confidence ranges for the parameters. The large sample approximation must be used. It is known that the asymptotic distribution of the MLE $\hat{\varphi}$ is $(\hat{\varphi} - \varphi) \to N\left(0, I^{-1}(\varphi)\right)$, where $I^{-1}(\varphi)$, and the inverse of the observed information matrix of the unknown parameters $\varphi = (\alpha, \beta)$ *is*:

$$I^{-1}(\varphi) = \left[\frac{\partial^2 L}{\partial \varphi^2}\right]^{-1}_{(\alpha,\beta)=(\hat{\alpha},\, \hat{\beta})} \tag{32}$$

and whose elements are given in the Appendix A.

4.2. ML_L Approach under R_aS_S

We assume $X_{(i)ic}$, $i = 1 \ldots m$ and $c = 1 \ldots k$ is an R_aS_S from the KMB_X model, which has sample size $n = mk$, where k is the number of cycles and m is the set size. We consider $Y_{ic} = X_{(i)ic}$ for simplicity, and for a given c, Y_{ic} is independent, with the pdf being equal to the pdf of the ith order statistics. The sample's L_L function $y_{1c}, y_{2c}, \ldots, y_{mc}$:

$$\begin{aligned}\ell_1 &= \prod_{c=1}^{k}\prod_{i=1}^{m}\tfrac{m!}{(i-1)!(m-i)!}[F(y_{ic})]^{i-1}f(y_{ic})[1-F(y_{ic})]^{m-i}\\ &= \prod_{c=1}^{k}\prod_{i=1}^{m}\tfrac{m!}{(i-1)!(m-i)!}\left[\tfrac{e}{e-1}\left(1-e^{-[Q_{ic}]^{\beta}}\right)\right]^{i-1}\tfrac{2e\beta\alpha^2}{e-1}y_{ic}\\ &\quad e^{-[(\alpha y_{ic})^2+[Q_{ic}]^{\beta}]}[Q_{ic}]^{\beta-1}\left[1-\tfrac{e}{e-1}\left(1-e^{-[Q_{ic}]^{\beta}}\right)\right]^{m-i},\end{aligned} \tag{33}$$

where $Q_{ic} = 1 - e^{-(\alpha y_{ic})^2}$. The log-$L_L$ function of the KMB_X distribution under R_aS_S is provided via:

$$\begin{aligned}\ln \ell_1 = \ln c + mk\ln\beta + 2mk\ln\alpha + \sum_{c=1}^{k}\sum_{i=1}^{m} ln(y_{ic}) - \sum_{c=1}^{k}\sum_{i=1}^{m}\left[(\alpha y_{ic})^2 + [Q_{ic}]^{\beta}\right] + (\beta-1)\sum_{c=1}^{k}\sum_{i=1}^{m} ln(Q_{ic})\\ + \sum_{c=1}^{k}\sum_{i=1}^{m}(i-1)ln\left[1-e^{-[Q_{ic}]^{\beta}}\right] + \sum_{c=1}^{k}\sum_{i=1}^{m}(m-i)ln\left[1-\tfrac{e}{e-1}\left(1-e^{-[Q_{ic}]^{\beta}}\right)\right].\end{aligned} \tag{34}$$

Differentiating Equation (34) partially with regard to α and β and equating the results to 0, we can solve the non-linear system of equations simultaneously. Then, we can get the ML_LE_s of parameters α and β symbolized by $\hat{\alpha}$ and $\hat{\beta}$, respectively, using the Mathematica (10) software program.

4.3. Numerical Outcomes

This subsection describes the numerical investigation used to derive the ML_LE_s of the population parameters for the KMB_X distribution using R_aS_S and S_iR_S. A comparative study is carried out by comparing estimates in terms of the $M_SE_{R_S}$, biases, and relative efficiency (R_EE_F). The following algorithm describes the simulation techniques.

First procedure: The R_S measuring n = 50, 150, 250, 500, and 1000 with m = n, $k = n$ are generated from KMB_X model, where $n^2 = m \times k$. After this, we rank one observation from each cycle.

Second procedure: The numerical values of the parameter are chosen.

Third procedure: The ML_LE_s are calculated under S_iR_S and R_aS_S for the given set of parameters and each n.

Fourth procedure: We repeat the above procedures from the first to third N times representing various samples, where N = 1000. After this, the B_Is, M_SE_Rs, and $R_EE_F = M_SE_R$ $(R_aS_S)/M_SE_R$ (S_iR_S) of the estimates are investigated.

Fifth procedure: Tables 1–6 provide the numerical results.

Table 1. The ML_LE_s, B_Is, M_SE_R, and R_EE_F of the KMB_X model under S_iR_S and R_aS_S at $\alpha = 0.9$, $\beta = 0.5$.

n	S_iR_S			R_aS_S			R_EE_F
	ML_LE	B_I	M_SE_R	ML_LE	B_I	M_SE_R	
50	0.96494	0.06494	0.02302	0.91408	0.01408	0.00364	0.15794
	0.56663	0.06663	0.02905	0.50424	0.00424	0.00272	0.09348
150	0.92564	0.02564	0.01394	0.89715	−0.00286	0.00096	0.06905
	0.49715	−0.00285	0.00801	0.49692	−0.00308	0.00080	0.09998
250	0.91592	0.01592	0.00439	0.90013	0.00013	0.00019	0.04265
	0.50587	0.00587	0.00286	0.50162	0.00162	0.00015	0.05289
500	0.90698	0.00698	0.00227	0.89978	−0.00022	0.00017	0.07597
	0.51065	0.01065	0.00179	0.49973	−0.00027	0.00014	0.07568
1000	0.89338	−0.00662	0.00087	0.89998	−0.00002	0.00003	0.03759
	0.49586	−0.00415	0.00052	0.50036	0.00036	0.00003	0.05376

Table 2. The ML_LE_s, B_Is, M_SE_R, and R_EE_F of the KMB_X model under S_iR_S and R_aS_S at $\alpha = 0.7$, $\beta = 1.2$.

n	S_iR_S			R_aS_S			R_EE_F
	ML_LE	B_I	M_SE_R	ML_LE	B_I	M_SE_R	
50	0.71199	0.01198	0.01641	0.69496	−0.00504	0.00204	0.12425
	1.23371	0.03371	0.07765	1.18874	−0.01126	0.01465	0.18867
150	0.70128	0.00128	0.00412	0.70341	0.00341	0.00052	0.12526
	1.21843	0.01843	0.05381	1.21744	0.01744	0.00486	0.09033
250	0.71035	0.01035	0.00281	0.69710	−0.00290	0.00014	0.05060
	1.21397	0.01397	0.01423	1.19018	−0.00982	0.00157	0.11022
500	0.70168	0.00168	0.00132	0.69931	−0.00070	0.00005	0.04155
	1.22349	0.02349	0.01004	1.19994	−0.00006	0.00076	0.07581
1000	0.70055	0.00055	0.00037	0.69965	−0.00036	0.00003	0.08976
	1.21896	0.01896	0.00504	1.20106	0.00106	0.00029	0.05743

Considering Tables 1–6, the relevant points should be noted:

- The B_Is and M_SE_Rs for the estimations depending on S_iR_S are greater than the comparable values depending on R_aS_S;
- In most scenarios, the B_Is and M_SE_R decrease as the *n* rises for both sampling strategies;
- In most cases, the efficiency of the estimates rises as the sample numbers grow;
- The ML_LE_s depending on R_aS_S have lower M_SE_R values than the corresponding values depending on S_iR_S.

Table 3. The ML_LE_s, B_Is, M_SE_R, and R_EE_F of the KMB_X model under S_iR_S and R_aS_S at $\alpha = 1.2$, $\beta = 0.8$.

n	S_iR_S			R_aS_S			R_EE_F
	ML_LE	B_I	M_SE_R	ML_LE	B_I	M_SE_R	
50	1.23291	0.03291	0.04986	1.22258	0.02258	0.00777	0.15578
	0.82114	0.02113	0.03598	0.82070	0.02070	0.00601	0.16693
150	1.20390	0.00390	0.02785	1.18876	−0.01124	0.00255	0.09166
	0.79966	−0.00034	0.01355	0.78934	−0.01066	0.00161	0.11864
250	1.23491	0.03491	0.00737	1.19494	−0.00506	0.00047	0.06430
	0.84220	0.04220	0.00967	0.79098	−0.00902	0.00064	0.06587
500	1.20088	0.00088	0.00600	1.19423	−0.00577	0.00034	0.05708
	0.79162	−0.00838	0.00618	0.79611	−0.00389	0.00029	0.04713
1000	1.19978	−0.00022	0.00228	1.19724	−0.00276	0.00010	0.04262
	0.81249	0.01249	0.00163	0.79893	−0.00107	0.00009	0.05454

Table 4. The ML_LE_s, B_Is, M_SE_R, and R_EE_F of the KMB_X model under S_iR_S and R_aS_S at $\alpha = 0.5$, $\beta = 0.5$.

n	S_iR_S			R_aS_S			R_EE_F
	ML_LE	B_I	M_SE_R	ML_LE	B_I	M_SE_R	
50	0.50285	0.00285	0.00512	0.50386	0.00386	0.00073	0.14321
	0.49913	−0.00087	0.01764	0.51884	0.01884	0.00570	0.32300
150	0.50529	0.00529	0.00230	0.50698	0.00698	0.00031	0.13363
	0.52127	0.02127	0.01639	0.51885	0.01885	0.00181	0.11041
250	0.51010	0.01010	0.00172	0.49867	−0.00133	0.00006	0.03632
	0.52292	0.02292	0.00740	0.49353	−0.00647	0.00037	0.04959
500	0.50559	0.00559	0.00056	0.50038	0.00037	0.00004	0.06248
	0.49469	−0.00531	0.00275	0.50102	0.00102	0.00018	0.06560
1000	0.50033	0.00033	0.00018	0.50046	0.00046	0.00001	0.06492
	0.50108	0.00108	0.00064	0.50163	0.00163	0.00008	0.12523

Table 5. The ML_LE_s, B_Is, M_SE_R, and R_EE_F of the KMB_X model under S_iR_S and R_aS_S at $\alpha = 1.5$, $\beta = 1.2$.

n	S_iR_S			R_aS_S			R_EE_F
	ML_LE	B_I	M_SE_R	ML_LE	B_I	M_SE_R	
50	1.59446	0.09446	0.11720	1.53348	0.03348	0.01638	0.13979
	1.35838	0.15838	0.15340	1.22161	0.02161	0.01185	0.07722
150	1.58630	0.08630	0.03646	1.47738	−0.02262	0.00338	0.09269
	1.26562	0.06562	0.03414	1.17926	−0.02074	0.00304	0.08898
250	1.52835	0.02836	0.01687	1.50914	0.00914	0.00086	0.05073
	1.22796	0.02796	0.01695	1.21189	0.01189	0.00083	0.04872
500	1.49492	−0.00508	0.00549	1.50226	0.00226	0.00058	0.10633
	1.18883	−0.01117	0.00662	1.20171	0.00171	0.00045	0.06753
1000	1.49477	−0.00523	0.00323	1.50460	0.00460	0.00017	0.05218
	1.20018	0.00018	0.00260	1.20380	0.00380	0.00015	0.05880

Table 6. The ML_LE_s, B_Is, M_SE_R, and R_EE_F of the KMB_X model under S_iR_S and R_aS_S at $\alpha = 0.8$, $\beta = 0.8$.

n	S_iR_S			R_aS_S			R_EE_F
	ML_LE	B_I	M_SE_R	ML_LE	B_I	M_SE_R	
50	0.88857	0.08857	0.02169	0.80473	0.00472	0.00224	0.10323
	0.85532	0.05532	0.03941	0.80765	0.00765	0.00443	0.11247
150	0.80340	0.00340	0.00942	0.80461	0.00461	0.00067	0.07145
	0.84545	0.04545	0.03142	0.80745	0.00745	0.00218	0.06927
250	0.82881	0.02881	0.00474	0.80171	0.00171	0.00015	0.03126
	0.82289	0.02289	0.01406	0.80072	0.00072	0.00064	0.04558
500	0.79461	−0.00539	0.00298	0.80089	0.00089	0.00008	0.02542
	0.79290	−0.00710	0.00643	0.80203	0.00203	0.00029	0.04512
1000	0.79628	−0.00372	0.00055	0.80068	0.00068	0.00005	0.09571
	0.79694	−0.00306	0.00153	0.79923	−0.00077	0.00020	0.13225

5. Application to Real Data Sets

Here, in this section, we demonstrate the usefulness of the KMB_X model by using three data sets. Numerous researchers have utilized these data to demonstrate the applicability of competing models. We additionally offer a formative assessment of the models' goodness of fit and draw comparisons with other continuous models that have one, two, three, four, five, and six parameters. The goodness of fit measures comprise the Akaike information criterion (INC) ($\mathcal{M}$**1**), consistent Akaike INC ($\mathcal{M}$**2**), Bayesian INC ($\mathcal{M}$**3**), and Hannan–Quinn INC ($\mathcal{M}$**4**), which are calculated in order to compare the fitted models. The smaller the values of these statistics, generally the superior the match to both data sets.

The First Data Set: Survival Times Data

The first data set was studied by Bjerkedal in 1960, representing the survival times (in days) of 72 guinea pigs infected with virulent tubercle bacilli. For these data, shall compared the ts of the KMB_X distribution with the exponential (E), Marshall–Olkin E (MO_LE), Burr X-E (B_XE), Kumaraswamy E (KE), beta E (BE), Kumaraswamy MO_LE (KMO_LE), generalized MO_LE (GMO_LE), MO_L Kumaraswamy E (MO_LKE), and moment E (ME) models (see Refaie 2018).

The Second Data Set: Relief Times Data

This set of data contained only the relief times of 20 patients who received an analgesic (Gross and Clark 1975). For these data, we compared the KMB_X distribution with the MO_LE, B_XE, KE, BE, KMO_LE, GMO_LE, Ailamujia (A) (Lv et al. 2002), inverse A (IA) (Aijaz et al. 2020), E, McDonald (M_C) log-logistic (M_CL_OL) (Tahir et al. 2014), M_CWeibull (M_CW) (Cordeiro et al. 2014), beta (B) generalized inverse Weibull geometric distribution (BGIWG) (Elbatal et al. 2017), B transmuted (T_R) Weibull (BT_RW) (Afify et al. 2017), new modified Weibull (NMW) (Almalki and Yuan 2013), T_R complementary Weibull-geometric (T_RCWG) (Afify et al. 2014), B Weibull (BW) (Lee et al. 2007), exponentiated T_R generalized Rayleigh (ET_RGR) (Ahmed et al. 2015), Weibull–Lomax (WL) (Tahir et al. 2015), T_R Weibull–Lomax (T_RWL) (Afify et al. 2015), Burr XII, Kumaraswamy–Weibull–exponential (KWE) (ZeinEldina and Elgarhyc 2018), Weibull (W), gamma-Chen (C_H) (GC_H) (Alzaatreh et al. 2014), beta-C_H (BC_H) (Eugene et al. 2002), Marshall–Olkin C_H (MOC_H) (Jose 2011), T_R Chen (T_RC_H) (Khan et al. 2013), T_R exponentiated C_H (T_REC_H) (Khan et al. 2016), and C_H distributions.

The Third Data Set: Financial Data

The third data set was studied by Mead in 2014, containing actual monthly tax revenues from Egypt from January 2006 to November 2010. For these data, we compared the KMB_X distribution with the B_X, E, MO_LE, exponentiated Weibull (EW), odd Weibull exponential (OWE), and Weibull (W) models. The profile log-likelihood plots are shown in Figures 3–5.

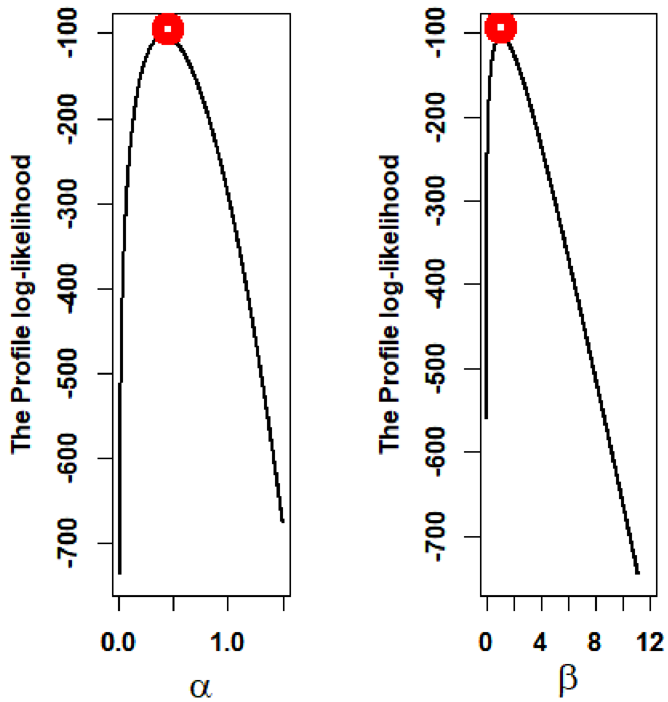

Figure 3. The profile log-likelihood plot for the first data set.

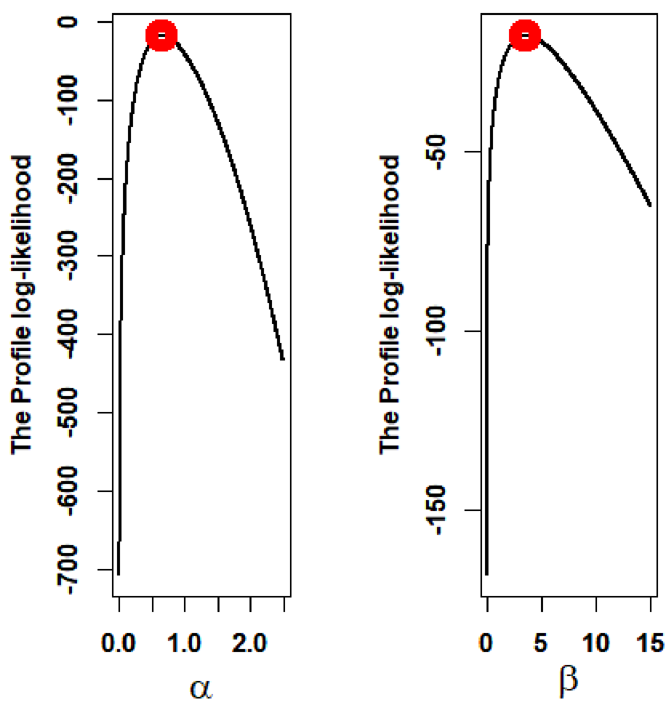

Figure 4. The profile log-likelihood plot for the second data set.

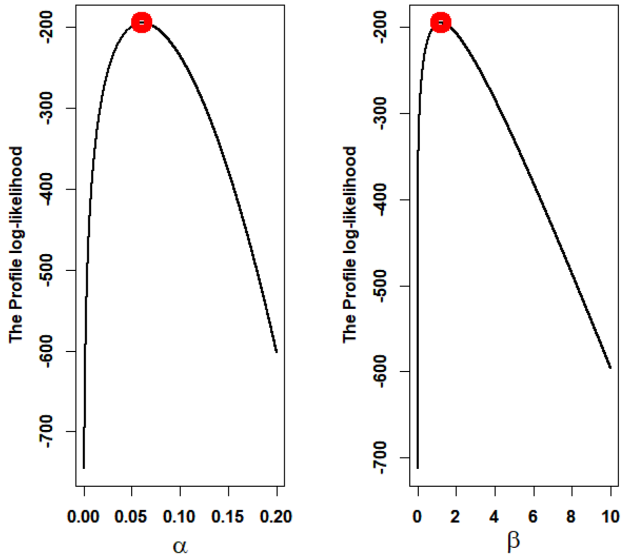

Figure 5. The profile log-likelihood plot for the third data set.

The estimated parameters along with their Ser values **and** the statistics for the fitted models are provided in Tables 7–12. We note from Table 8, Table 10, and Table 12 that the KMB_X gives the smallest values of $\mathcal{M}1$, $\mathcal{M}2$, $\mathcal{M}3$, and $\mathcal{M}4$ as compared to the other competitive models. Therefore, the KMB_X distribution provides the best t for the three data sets. More information can be found in Figures 6–8.

Table 7. Numerical values of ML_LE_s and (SErs) for the first data set.

Models	ML_LE_s and SErs			
KMB_X (α, β)	0.443 (0.038)	1.081 (0.153)		
KMO_LE (α, μ, τ, β)	0.373 (0.136)	3.478 (0.862)	3.306 (0.781)	0.299 (1.113)
B_XE (θ, β)	0.475 (0.06)	0.206 (0.012)		
GMO_LE (λ, α, β)	0.179 (0.07)	47.640 (44.90)	4.47 (1.33)	
BE (μ, τ, β)	0.807 (0.70)	3.461 (1.003)	1.3311 (0.8551)	
KE (μ, τ, β)	3.304 (1.1061)	1.1 (0.76)	1.037 (0.614)	
MO_LKE (α, μ, τ, β)	0.01 (0.002)	2.7162 (1.3158)	1.99 (0.784)	0.099 (0.05)
MO_LE (α, β)	8.778 (3.555)	1.3788 (0.1929)		
ME (β)	0.925 (0.077)			
E (β)	0.540 (0.06)			

Table 8. Numerical values of $\mathcal{M}1$, $\mathcal{M}2$, $\mathcal{M}3$, and $\mathcal{M}4$ for the first data set.

Models	$\mathcal{M}1$	$\mathcal{M}2$	$\mathcal{M}3$	$\mathcal{M}4$
KMB_X	193.494	194.2	193.209	195.307
KMO_LE	207.82	216.94	208.42	211.42
B_XE	235.30	239.90	235.50	237.10
GMO_LE	210.54	217.38	210.89	213.24
BE	207.38	214.22	207.73	210.08
KE	209.42	216.24	209.77	212.12
MO_LKE	209.44	218.56	210.04	213.04
MO_LE	210.36	214.92	210.53	212.16
ME	210.40	212.68	210.45	211.30
E	234.63	236.91	234.68	235.54

Table 9. Numerical values of ML_LE_s and (SErs) for the second data set.

Models	ML_LE_s and (SErs)					
KMB_X (α, β)	0.655 (0.085)	3.563 (2.431)		-	-	-
BGIWG (α, γ, θ, p, μ, τ)	19.187 (33.03)	20.597 (43.24)	1.435 (0.84)	9.85 (2.001)	39.231×10^{-5} (63.25)	5.802 (4.35)
MO_LE (α, β)	54.474 (35.581)	2.32 (0.374)				
B_XE (θ, β)	1.164 (0.33)	0.321 (0.030)				
KE (μ, τ, β)	83.76 (42.361)	0.57 (0.326)	3.333 (1.188)			
GMO_LE (λ, α, β)	0.52 (0.256)	89.462 (66.28)	3.169 (0.772)			
BE (μ, τ, β)	81.633 (120.41)	0.542 (0.327)	3.514 (1.410)			
KMO_LE (α, μ, τ, β)	8.87 (9.15)	34.83 (22.31)	0.299 (0.24)	4.90 (3.18)		
A (β)	0.95 (0.15)					
IA (β)	3.45 (0.55)					
E (β)	0.53 (0.12)					
KWE (μ, τ, α, β, λ)	7.820 (3.992)	21.52 (0.10)	1.47 (1.022)	0.402 (0.362)	0.005 (0.002)	
BT_RW(α, β, μ, τ, λ)	5.619 (9.35)	0.531 (0.15)	53.344 (111.45)	3.568 (4.27)	−0.772 (3.894)	-
M_CL_OL (α, β, μ, τ, c)	0.881 (0.11)	2.07 (3.69)	19.23 (22.34)	32.03 (43.08)	1.93 (5.17)	-
M_CW (α, β, μ, τ, c)	2.7738 (6.38)	0.3802 (0.188)	79.108 (119.131)	17.8976 (39.511)	3.0063 (13.968)	-
T_REC_H (α, β, μ, τ)	300.01 (587.04)	0.50 (0.56)	2.43 (1.08)	0.34 (0.11)		

Table 9. *Cont.*

Models	ML_LE_s and (SErs)					
T_RCWG (α, β, γ, λ)	43.663 (45.46)	5.127 (0.814)	0.282 (0.042)	−0.271 (0.66)	-	-
C_H (μ, τ)	0. 14 (0.05)	0.95 (0.09)			-	-
ET_RGR(α, β, λ, δ)	0.103 (0.44)	0.692 (0.09)	−0.342 (1.97)	23.54 (105.37)	-	-
T_RWL(μ, τ, β, θ, λ)	8.619 (42.83)	6.215 (4.501)	0.248 (0.67)	0.226 (0.202)	0.697 (0.338)	
WL(μ, τ, θ, λ)	14.74 (64.67)	5.585 (3.84)	0.263 (0.67)	0.22 (0.184)		
BXII (λ, θ)	0.016 (0.038)	103.60 (245.14)				
NMW (α, β, γ, δ, θ)	0.122 (0.06)	2.784 (20.37)	8.23×10^{-5}(0.151)	0.0003 (0.025)	2.79 (0.43)	-
W (λ, θ)	0.0021 (0.0004)	1.435 (0.0602)				
GC_H (α, β, μ, τ)	7.59 (2.09)	1.99 (0.46)	5.00 (1.07)	0.53 (0.003)		
BW (α, β, μ, τ)	0.831 (0.954)	0.613 (0.34)	29.95 (40.413)	11.632 (21.9)		
BC_H (α, β, μ, τ)	85.87 (103.13)	0.48 (0.51)	2.01 (0.69)	0.55 (0.20)		
MO_LC_H (α, μ, τ)	400.01 (488.06)	2.32 (0.64)	0.43 (0.08)			
T_RC_H (α, μ, τ)	0.75 (0.28)	0.07 (0.03)	1.02 (0.09)			

Table 10. Numerical values of $\mathcal{M}1$, $\mathcal{M}2$, $\mathcal{M}3$, and $\mathcal{M}4$ for the second data set.

Model	$\mathcal{M}1$	$\mathcal{M}2$	$\mathcal{M}3$	$\mathcal{M}4$
KMB_X	39.283	39.989	37.885	39.671
BGIWG	43.854	48.14	40.359	44.826
MO_LE	43.51	45.51	44.22	43.90
B_XE	48.10	50.10	48.80	48.50
KE	41.78	44.75	43.28	42.32
GMO_LE	42.75	45.74	44.25	43.34
BE	43.48	46.45	44.98	44.02
KMO_LE	42.80	46.84	45.55	43.60
A	54.32	55.31	54.54	54.50
IA	53.653	53.888	52.954	53.847
E	67.67	68.67	67.89	67.87
KWE	41.8619	46.1476	42.8337	46.8405
BT_RW	43.662	50.124	39.468	44.828
M_CL_OL	43.051	47.337	39.556	44.023
M_CW	43.854	48.14	40.359	44.826
T_REC_H	39.56	42.227	36.764	40.338
T_RCWG	51.173	55.459	47.678	52.145
C_H	53.14	53.846	51.742	53.529

Table 10. *Cont.*

Model	$\mathcal{M}1$	$\mathcal{M}2$	$\mathcal{M}3$	$\mathcal{M}4$
ET_RGR	42.396	45.063	39.6	43.174
T_RWL	47.804	52.09	44.309	48.776
WL	47.261	49.928	44.465	48.039
BXII	46.414	47.12	45.016	46.803
NMW	43.907	48.193	40.412	44.879
W	45.1728	45.8786	45.5615	47.1642
GC_H	46.35	49.017	43.554	47.128
BW	41.607	44.274	38.811	42.385
BC	40.51	43.177	37.714	41.288
MO_LC_H	44.88	46.38	42.783	45.463
T_RC_H	53.63	55.13	51.533	54.213

Table 11. Numerical values of ML_LE_s and (SErs) for the third data set.

Models	ML_LE_s and SErs		
KMB_X (α, β)	0.061 (0.006)	1.204 (0.195)	
B_X (α, β)	0.0644 (0.006)	1.0310 (0.184)	
EW (α, β, a)	1.548 (0.913)	0.471 (0.131)	88.690 (8.407)
OWE (α, a, b)	0.016 (0.019)	6.616 (5.444)	1.547 (1.563)
MO_LE (α, a)	0.209 (0.031)	11.565 (5.202)	
W (α, β)	0.007 (0.003)	1.822 (0.134)	
E (β)	0.074 (0.010)		

Table 12. Numerical values of $\mathcal{M}1$, $\mathcal{M}2$, $\mathcal{M}3$, and $\mathcal{M}4$ for the third data set.

Models	$\mathcal{M}1$	$\mathcal{M}2$	$\mathcal{M}3$	$\mathcal{M}4$
KMB_X	394.464	394.678	394.006	396.086
B_X	399.393	399.607	403.548	401.015
EW	538.535	538.979	544.716	540.942
OWE	404.876	405.313	411.109	407.309
MO_LE	552.738	552.956	556.859	554.343
W	398.593	398.808	402.749	400.215
E	611.935	612.006	613.995	612.737

Based on the numerical results acquired in Table 8, Table 10, and Table 12, we found that our model had the lowest values for $\boldsymbol{\mathcal{M}1}$, $\boldsymbol{\mathcal{M}2}$, $\boldsymbol{\mathcal{M}3}$, and $\boldsymbol{\mathcal{M}4}$. Figures 6–8 all supported these numerical results, showing that the KMB_X model is the best model for fitting the three data sets.

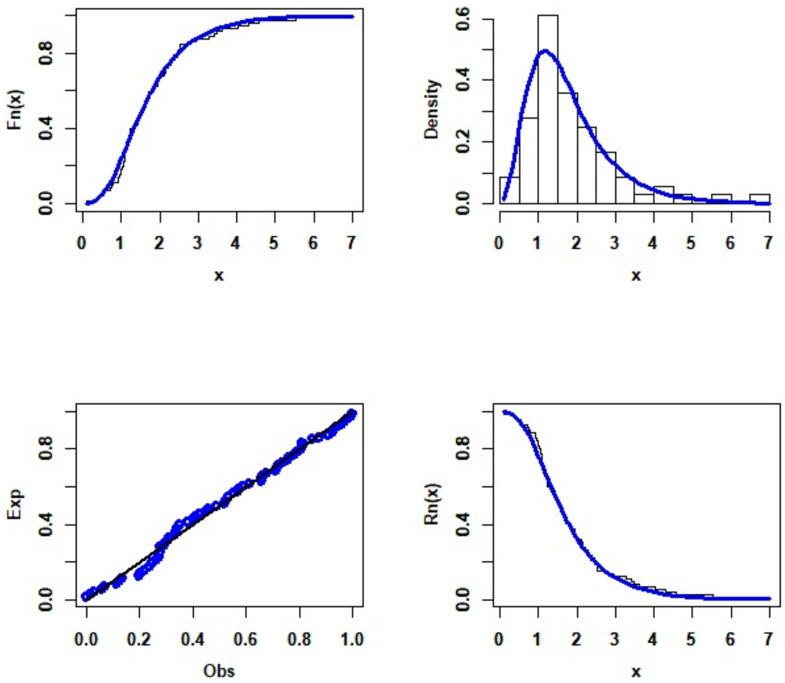

Figure 6. The fitted cdf, pdf, and pp plots and the estimated plot for the first data set.

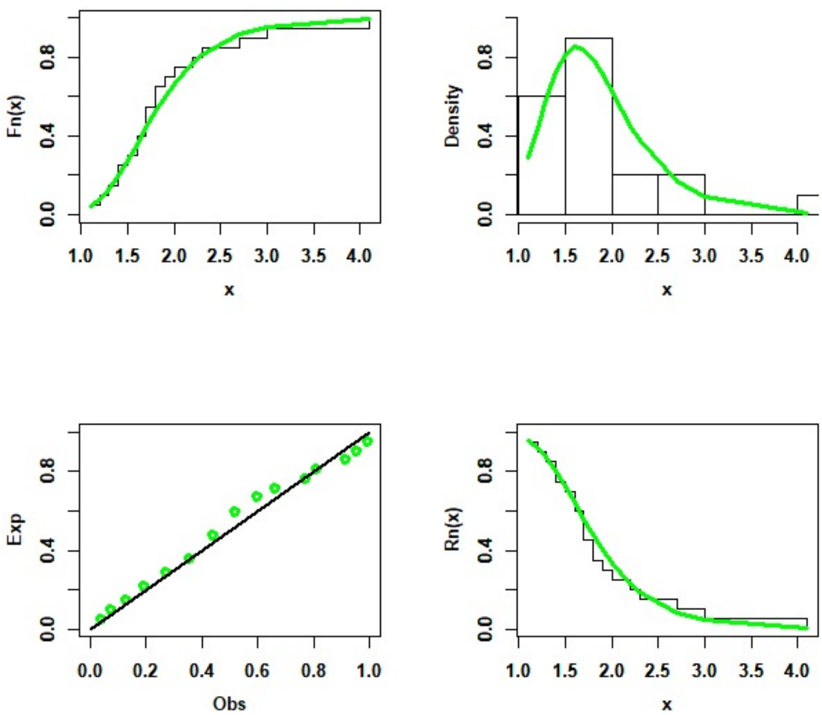

Figure 7. The fitted cdf, pdf, and pp plots and the estimated plot for the second data.

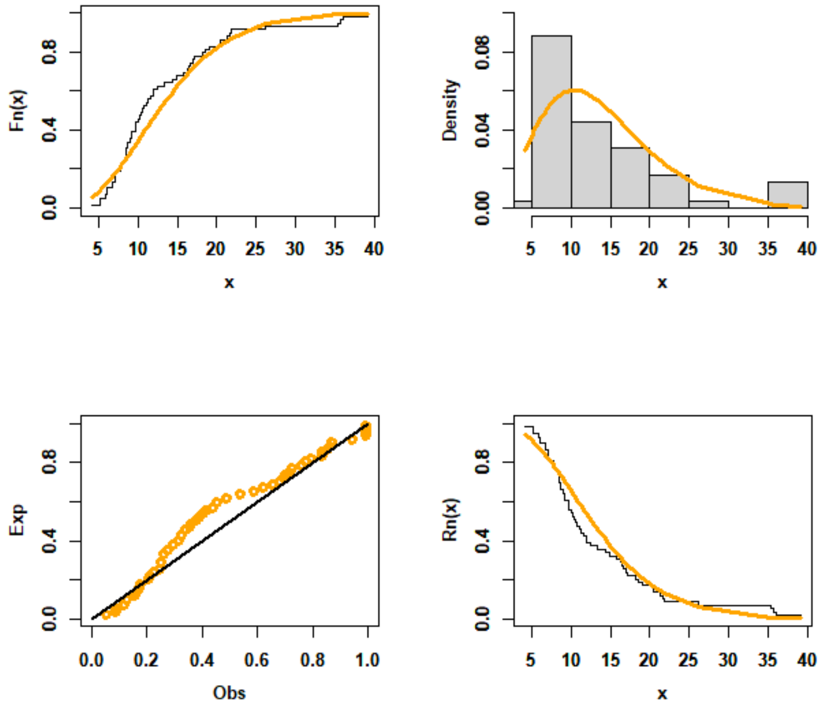

Figure 8. The fitted cdf, pdf, and pp plots and the estimated plot for the third data.

6. Actuarial Measures

In this part, we compute certain key risk measures for the recommended distribution, such as the value at risk and conditional value at risk, which are vital for strategy optimization despite uncertainty.

6.1. Value at Risk

If X $\sim$ KMB_X denotes a random variable with the cdf from (10), then its value at risk is:

$$\boldsymbol{RV_\nu} = -\frac{\mathbf{1}}{\boldsymbol{\alpha}}\boldsymbol{log}\left\{\mathbf{1} - \left[-\mathbf{log}\left(\mathbf{1} - \boldsymbol{\nu}\left(\mathbf{1} - \boldsymbol{e}^{-\mathbf{1}}\right)\right)\right]^{\frac{1}{\beta}}\right\}^{\frac{1}{2}}. \tag{35}$$

6.2. Conditional Value at Risk

Instead of using the value at risk, Artzner (1997, 1999) suggested using the conditional value at risk. The conditional value at risk is typically used to calculate the mean loss in cases where the value at risk exceeds the nominal values by a significant amount. The next expression serves as its definition:

$$CRV_\nu = \frac{1}{\nu}\int_0^\nu RV_\nu d\nu, \qquad 0 < \nu < 1. \tag{36}$$

The conditional value at risk of the KMB_X is provided via:

$$CRV_\nu = \frac{1}{\nu}\int_0^\nu = -\frac{1}{\alpha}log\left\{1 - \left[-\mathbf{log}\left(\mathbf{1} - \boldsymbol{\nu}\left(\mathbf{1} - \boldsymbol{e}^{-1}\right)\right)\right]^{\frac{1}{\beta}}\right\}^{\frac{1}{2}} d\nu, \qquad 0 < \nu < 1. \tag{37}$$

7. Conclusions

In this research, we investigated the Kavya–Manoharan–Burr X (KMB_X) model, which has two parameters. Its statistical and mathematical features (Q_U function, median, M_Os, incomplete M_Os, M_O-generating function, conditional M_Os, mean residual lifetime, and Rényi entropy) were derived. Based on S_iR_S and R_aS_S, the model parameters were estimated using the ML_L method. A simulation experiment was used to compare these estimators based on the B_I, M_SE_R, and efficiency. The relevance and flexibility of the KMB_X model were demonstrated using three real data sets. The new suggested model was superior to some well-known models in the modeling of the proposed data. We compared our model with twenty-nine other models, and our model gave the best fit for the data. Some useful actuarial risk measures, such as the value at risk and conditional value at risk, were also discussed.

Author Contributions: Conceptualization, O.H.M.H. and I.E.; methodology, A.H.A.-N.; software, M.E.; validation, O.H.M.H. and I.E.; formal analysis A.H.A.-N.; investigation, A.H.A.-N.; resources, A.H.A.-N.; data curation, M.E.; writing—original draft preparation, M.E.; writing—review and editing, O.H.M.H. and I.E.; visualization, O.H.M.H.; supervision, O.H.M.H. and I.E.; project administration, A.H.A.-N.; funding acquisition, O.H.M.H. All authors have read and agreed to the published version of the manuscript.

Funding: The authors appreciate The Deanship of Scientific Research, Vice Presidency for Graduate Studies and Scientific Research, King Faisal University, Saudi Arabia, grant no. 846.

Data Availability Statement: The data used to support the findings of this study are available from the corresponding author upon request.

Acknowledgments: The authors appreciate The Deanship of Scientific Research, Vice Presidency for Graduate Studies and Scientific Research, King Faisal University, Saudi Arabia, grant no. 846.

Conflicts of Interest: The authors declare no conflict of interest.

Appendix A

The second-order partial derivatives of the log-likelihood function of the KMB_X with respect to α, β are given by:

$$\frac{\partial^2 L}{\partial \alpha^2} = \frac{-2n}{\alpha^2} - 2\sum_{i=1}^{n} x_i - 2\beta \sum_{i=1}^{n} x_i^2 e^{-(\alpha x_i)^2}\left[1-e^{-(\alpha x_i)^2}\right]^{\beta-1} + 4\alpha^2\beta \sum_{i=1}^{n} x_i^4 e^{-(\alpha x_i)^2}\left[1-e^{-(\alpha x_i)^2}\right]^{\beta-1} - 4\alpha^2\beta(\beta-1)\sum_{i=1}^{n} x_i^4 e^{-2(\alpha x_i)^2}\left[1-e^{-(\alpha x_i)^2}\right]^{\beta-1} + (\beta-1)\sum_{i=1}^{n} \frac{2x_i^2\left(e^{(\alpha x_i)^2}-1\right)-4\alpha^2 x_i^4 e^{(\alpha x_i)^2}}{\left(e^{(\alpha x_i)^2}-1\right)^2}, \tag{A1}$$

$$\frac{\partial^2 L}{\partial \alpha \partial \beta} = 2\alpha\beta \sum_{i=1}^{n} x_i^2 e^{-(\alpha x_i)^2}\left[1-e^{-(\alpha x_i)^2}\right]^{\beta-1} \log\left[1-e^{-(\alpha x_i)^2}\right] + \sum_{i=1}^{n} \frac{2\alpha x_i^2\left[1-e^{-(\alpha x_i)^2}\right]^{\beta}}{e^{(\alpha x_i)^2}-1} + \sum_{i=1}^{n} \frac{2\alpha x_i^2}{e^{(\alpha x_i)^2}-1}. \tag{A2}$$

and:

$$\frac{\partial^2 L}{\partial \beta^2} = \frac{-n}{\beta^2} - \sum_{i=1}^{n}\left[1-e^{-(\alpha x_i)^2}\right]^{\beta}\left(\log\left[1-e^{-(\alpha x_i)^2}\right]\right)^2. \tag{A3}$$

References

Afify, Ahmed Z., Zohdy M. Nofal, and Nadeem Shafique Butt. 2014. Transmuted complementary Weibull geometric distribution. *Pakistan Journal of Statistics and Operations Research* 10: 435–54. [CrossRef]

Afify, Ahmed Z., Zohdy M. Nofal, Haitham M. Yousof, Yehia M. El Gebaly, and Nadeem Shafique Butt. 2015. Transmuted Weibull Lomax distribution. *Pakistan Journal of Statistics and Operations Research* 11: 135–52. [CrossRef]

Afify, Ahmed, Haitham Yousof, and Saralees Nadarajah. 2017. The beta transmuted-H family for lifetime data. *Statistics and Its Interface* 10: 505–20. [CrossRef]

Ahmed, Z., Zohdy M. Nofal, and N. Ebraheim Abd El Hadi. 2015. Exponentiated transmuted generalized Rayleigh distribution: A new four parameter Rayleigh distribution. *Pakistan Journal of Statistics and Operations Research* 11: 115–34.

Aijaz, Ahmad, Afaq Ahmad, and Rajnee Tripathi. 2020. Inverse Analogue of Ailamujia Distribution with Statistical Properties and Applications. *Asian Research Journal of Mathematics* 16: 36–46. [CrossRef]

Algarni, Ali, Abdullah M. Almarashi, I. Elbatal, Amal S. Hassan, Ehab M. Almetwally, Abdulkader M. Daghistani, and Mohammed Elgarhy. 2021. Type I half logistic Burr XG family: Properties, Bayesian, and non-Bayesian estimation under censored samples and applications to COVID-19 data. *Mathematical Problems in Engineering* 2021: 5461130. [CrossRef]

Almalki, Saad J., and Jingsong Yuan. 2013. A new modified Weibull distribution. *Reliability Engineering and System Safety* 111: 164–70. [CrossRef]

Alotaibi, Naif, Atef F. Hashem, Ibrahim Elbatal, Salem A. Alyami, A. S. Al-Moisheer, and Mohammed Elgarhy. 2022a. Inference for a Kavya–Manoharan Inverse Length Biased Exponential Distribution under Progressive-Stress Model Based on Progressive Type-II Censoring. *Entropy* 24: 1033. [CrossRef]

Alotaibi, Naif, Ibrahim Elbatal, Ehab M. Almetwally, Salem A. Alyami, A. S. Al-Moisheer, and Mohammed Elgarhy. 2022b. Bivariate Step-Stress Accelerated Life Tests for the Kavya–Manoharan Exponentiated Weibull Model under Progressive Censoring with Applications. *Symmetry* 14: 1791. [CrossRef]

Aludaat, K. M., Moh'D Taleb Alodat, and Tareq Alodat. 2008. Parameter estimation of Burr type X distribution for grouped data. *Applied Mathematical Sciences* 2: 415–23.

Alzaatreh, Ayman, Felix Famoye, and Carl Lee. 2014. The gamma-normal distribution: Properties and applications. *Computational Statistics and Data Analysis* 69: 67–80. [CrossRef]

Artzner, Philippe. 1997. Thinking Coherently. *Risk* 10: 68–71.

Artzner, Philippe. 1999. Application of coherent risk measures to capital requirements in insurance. *North American Actuarial Journal* 3: 11–25. [CrossRef]

Bantan, Rashad A. R., Christophe Chesneau, Farrukh Jamal, Ibrahim Elbatal, and Mohammed Elgarhy. 2021. The Truncated Burr X-G Family of Distributions: Properties and Applications to Actuarial and Financial Data. *Entropy* 23: 1088. [CrossRef] [PubMed]

Burr, Irving W. 1942. Cumulative frequency functions. *The Annals of Mathematical Statistics* 13: 215–32. [CrossRef]

Cordeiro, Gauss M., Elizabeth M. Hashimoto, and Edwin M. M. Ortega. 2014. The McDonald Weibull model. *Statistics* 48: 256–78. [CrossRef]

Elbatal, I., Yehia M. El Gebaly, and Essam A. Amin. 2017. The beta generalized inverse Weibull geometric distribution and its applications. *Pakistan Journal of Statistics and Operation Research* 13: 75–90. [CrossRef]

El-Morshedy, M., Ziyad Ali Alhussain, Doaa Atta, Ehab M. Almetwally, and M. S. Eliwa. 2020. Bivariate Burr X generator of distributions: Properties and estimation methods with applications to complete and type-II censored samples. *Mathematics* 8: 264. [CrossRef]

Eugene, Nicholas, Carl Lee, and Felix Famoye. 2002. Beta-normal distribution and its applications. *Communications in Statistics-Theory and Methods* 31: 497–512. [CrossRef]

Gross, Alan J., and Virginia Clark. 1975. *Survival Distributions: Reliability Applications in the Biomedical Sciences*. New York: John Wiley and Sons.

Jose, K. K. 2011. Marshall-Olkin family of distributions and their applications in reliability theory, time series modeling and stress-strength analysis. Paper presented at ISI 58th World Statistics Congress International Statistical Institute, Dublin, Ireland, August 21–26; pp. 3918–23.

Kavya, P., and M. Manoharan. 2020. On a Generalized lifetime model using DUS transformation. In *Applied Probability and Stochastic Processes*. Infosys Science Foundation Series. Edited by V. Joshua, S. Varadhan and V. Vishnevsky. Singapore: Springer, pp. 281–91.

Kavya, P., and M. Manoharan. 2021. Some parsimonious models for lifetimes and applications. *Journal of Statistical Computation and Simulation* 91: 3693–708. [CrossRef]

Khan, Muhammad Shuaib, Robert King, and Irene Hudson. 2013. A new three parameter transmuted Chen lifetime distribution with application. *Journal of Applied Statistical Science* 21: 239–59.

Khan, Muhammad Shuaib, Robert King, and Irene Lena Hudson. 2016. Transmuted exponentiated Chen distribution with application to survival data. *ANZIAM Journal* 57: 268–90. [CrossRef]

Kumar, Dinesh, Umesh Singh, and Sanjay Kumar Singh. 2015. A method of proposing new distribution and its application to bladder cancer patients data. *Journal of Statistics Applications and Probability Letters* 2: 235–45.

Lee, Carl, Felix Famoye, and Olugbenga Olumolade. 2007. Beta-Weibull distribution: Some properties and applications to censored data. *Journal of Modern Applied Statistical Methods* 6: 173–86. [CrossRef]

Lv, H. Q., L. H. Gao, and C. L. Chen. 2002. Ailamujia distribution and its application in support ability data analysis. *Journal of Academy of Armored Force Engineering* 16: 48–52.

Raqab, Mohammad Z., and Debasis Kundu. 2006. Burr type X distribution: Revisited. *Journal of Probability and Statistical Sciences* 4: 179–93.

Refaie, Mohamed K. A. 2018. Burr X exponentiated exponential distribution. *Journal of Statistics and Applications* 1: 71–88.

Surles, J. G., and W. J. Padgett. 2001. Inference for reliability and stress-strength for a scaled Burr type X distribution. *Lifetime Data Analysis* 7: 187–200. [CrossRef]

Surles, J. G., and W. J. Padgett. 2005. Some properties of a scaled Burr type X distribution. *Journal of statistical planning and inference* 128: 271–80. [CrossRef]

Tahir, Muhammad H., Gauss M. Cordeiro, M. Mansoor, and Muhammad Zubair. 2015. The Weibull-Lomax distribution: Properties and applications. *Hacettepe Journal of Mathematics and Statistics* 44: 455–74. [CrossRef]

Tahir, Muhammad Hussain, Muhammad Mansoor, Muhammad Zubair, and Gholamhossein Hamedani. 2014. McDonald log logistic distribution with an application to breast cancer data. *Journal of Statistical Theory and Applications* 13: 65–82. [CrossRef]

ZeinEldina, Ramadan A., and M. Elgarhyc. 2018. A new generalization of Weibull-exponential distribution with application. *Journal of Nonlinear Science and Applications* 11: 1099–112. [CrossRef]